JOURNAL OF VIROLOGY, Sept. 2006, p. 8469–8481 Vol. 80, No. 17
0022-538X/06/$08.00+0 doi:10.1128/JVI.02749-05


# Differences and Similarities in Viral Life Cycle Progression and Host Cell Physiology after Infection of Human Dendritic Cells with Modified Vaccinia Virus Ankara and Vaccinia Virus

Ann Chahroudi,[1] David A. Garber,[1] Patrick Reeves,[2] Luzheng Liu,[1]†
Daniel Kalman,[2] and Mark B. Feinberg[1]*‡

*Emory Vaccine Center[1] and Division of Pathology and Laboratory Medicine,[2]*
*Emory University School of Medicine, Atlanta, Georgia 30329*

Received 31 December 2005/Accepted 17 May 2006

**Modified vaccinia virus Ankara (MVA) is an attenuated strain of vaccinia virus (VV) that has attracted significant attention as a candidate viral vector vaccine for immunization against infectious diseases and treatment of malignancies. Although MVA is unable to replicate in most nonavian cells, vaccination with MVA elicits immune responses that approximate those seen after the administration of replication-competent strains of VV. However, the mechanisms by which these viruses elicit immune responses and the determinants of their relative immunogenicity are incompletely understood. Studying the interactions of VV and MVA with cells of the human immune system may elucidate these mechanisms, as well as provide a rational basis for the further enhancement of the immunogenicity of recombinant MVA vectors. Toward this end, we investigated the consequences of MVA or VV infection of human dendritic cells (DCs), key professional antigen-presenting cells essential for the generation of immune responses. We determined that a block to the formation of intracellular viral replication centers results in abortive infection of DCs with both VV and MVA. MVA inhibited cellular protein synthesis more rapidly than VV and displayed a distinct pattern of viral protein expression in infected DCs. MVA also induced apoptosis in DCs more rapidly than VV, and DC apoptosis after MVA infection was associated with an accelerated decline in the levels of intracellular Bcl-2 and Bcl-$X_L$. These findings suggest that antigen presentation pathways may contribute differentially to the immunogenicity of VV and MVA and that targeted modifications of virus-induced DC apoptosis may further increase the immunogenicity of MVA-vectored vaccines.**

Vaccinia virus (VV) and the attenuated modified vaccinia virus Ankara (MVA) are members of the family *Poxviridae* and the genus *Orthopoxvirus*. They are large (167 to 224 kbp), double-stranded DNA viruses that replicate in the cytoplasm of infected host cells (51). MVA was derived by more than 500 passages of the Ankara strain of VV on chicken embryo fibroblasts (32, 46). During this extensive passage, six regions totaling 31 kb were lost from the VV genome, resulting in the deletion of a number of host-range restriction and immunomodulatory genes (4, 6). As a result of the deletion of genes involved in host-range restriction, replication of MVA in most nonavian cell types aborts at a late stage of the virus life cycle (16, 47, 67).

VV is a potently immunogenic vaccine for smallpox, a disease caused by infection with the orthopoxvirus variola, and induces long-term humoral and cell-mediated immune responses (19, 31). Due to VV-related complications (primarily observed in children and the immunocompromised), the use of alternative vaccines, such as MVA, was investigated toward the end of the smallpox eradication campaign. Approximately 120,000 individuals were immunized with MVA in Germany and Turkey, and no adverse effects were recorded, even in those at high risk for complications of standard VV-based vaccines (47). Interestingly, despite the fact that MVA is unable to replicate in human cells, a number of recent studies have found that the immunogenicity of MVA is equal to or greater than that of replication-competent strains of VV (18, 24, 29, 57). Due to its safety and immunogenicity, MVA is now a proposed candidate vaccine vector for immunization against human immunodeficiency virus, malaria, tuberculosis, and weaponized smallpox and for immunotherapy for a variety of malignant diseases (5, 22, 24, 48, 49, 52, 64). Further improvement of MVA-vectored vaccines is needed, however, since studies in macaques have demonstrated appreciable immune responses only to immunodominant epitopes (62). Furthermore, disappointing levels of immunogenicity against inserted gene products have been observed in human clinical trials of recombinant MVA (52, 64a).

Surprisingly, little information exists as to the mechanisms by which immune responses to VV or MVA are generated or why the immunogenicity of MVA may approximate or exceed that of VV despite being replication defective in human (as well as murine and nonhuman primate) cells. We have previously investigated the cellular tropism of VV for primary hematolymphoid cells that are essential for the generation of cellular and humoral immune responses and found that the

* Corresponding author. Mailing address: Merck Vaccine Division, Merck & Co., Inc., WP97-A337, 770 Sumneytown Pike, P.O. Box 4, West Point, PA 19486. Phone: (215) 652-8664. Fax: (215) 652-8918. E-mail: mark_feinberg@merck.com.

† Present address: Harvard Skin Disease Research Center, Department of Dermatology, Brigham and Women's Hospital, Boston, MA 02115.

‡ Present address: Merck Vaccine Division, West Point, PA 19486.

myeloid and plasmacytoid dendritic cell (DC) subsets are preferential targets for infection in both humans and mice (17; L. Liu et al., unpublished data). DCs are the most potent antigen-presenting cells (APCs) and are the only cell type capable of activating naive T cells (10, 40). DCs are specialized to process and present antigen (Ag) synthesized endogenously as a consequence of viral infection (direct presentation) or exogenously via Ag capture from the extracellular compartment (cross-presentation) (50, 63). Cross-presentation may be particularly important to generate immunity to viruses that either do not infect DCs or that inhibit their Ag-presenting capabilities (54).

VV infection of DCs is abortive and is characterized by early, but not late, viral gene expression (12, 23, 25, 35, 66) and the absence of viral DNA accumulation (23). However, the precise reason for the abortive infection of DCs with VV or the precise stage at which the infection aborts is not known. Although a late block to virion assembly is believed to explain the nonproductive infection of nonavian cells with MVA (28, 60, 67), the stage at which the MVA replication cycle is aborted in human DCs has not previously been assessed. In the present study, we sought to investigate the specific nature of the block to VV replication in DCs and to determine whether MVA infection of DCs aborts at a similar stage. The discrete, progressive stages of orthopoxvirus replication have been described in detail (reviewed in reference 51). Briefly, after virus entry, early genes are transcribed, leading to the expression of a number of molecules necessary for viral DNA synthesis, which occurs in a juxtanuclear factory area, or replication center, enclosed by rough endoplasmic reticulum (70). Intermediate and late viral genes, including structural proteins, enzymes, and early transcription factors, are then transcribed. Viral DNA is incorporated into immature virions (IV) that mature into infectious intracellular mature virions (IMV), some of which are wrapped by a double membrane derived from the *trans*-Golgi to form intracellular enveloped virions (IEV). At the cell surface, IEV fuse with the host cell membrane, lose their outer membrane, and form cell-associated enveloped virions (CEV). CEV become extracellular enveloped virions by detaching from the cell membrane directly or by inducing actin polymerization and detaching from the tips of actin-filled microvilli.

To successfully replicate in infected cells, many viruses have evolved factors that interfere with cellular apoptotic pathways since the initiation of apoptosis early in infection may limit the production of viral progeny (7). Apoptosis is a highly regulated mechanism of cell death that is mediated by a family of cysteine proteases, or caspases, whose activation is triggered by a number of signals, including ligation of cell surface death receptors and depolarization of the mitochondrial membrane (69). VV and MVA encode factors that inhibit mitochondrial depolarization (F1L [74]) and type I interferon [IFN]-induced apoptosis (E3L [42]); in addition, VV (but not MVA [6]) encodes B13R that has been shown to inhibit the death receptor-mediated activation of caspase 8 (21, 37). Still, both VV and MVA have been shown to induce apoptosis of human DCs (25, 66, 71), although several important questions remain. (i) What is the trigger for orthopoxvirus-induced DC apoptosis? (ii) Do VV and MVA induce DC apoptosis in the same way and with the same kinetics? (iii) Is the abortive nature of DC infection with VV (and perhaps MVA) due to the induction of apoptosis in the course of viral life cycle progression? (iv) Is DC apoptosis a survival strategy of the virus or host? (v) How does DC apoptosis contribute to or antagonize the generation of antiviral immune responses?

To address these questions, we carefully examined, both quantitatively and by direct visualization, the extent of VV and MVA replication in DCs and the virus-induced cytopathic effect. A direct comparison of the consequences of DC infection with these two viruses has not previously been performed and may be important for elucidating the mechanisms of anti-orthopoxviral immunity, as well as for the rational design of orthopoxvirus-vectored vaccines that exhibit optimal immunogenicity. We found that the infection of DCs with either VV or MVA aborts prior to the formation of viral replication centers and before the induction of apoptosis. We further observed that in MVA-infected DCs apoptosis is initiated at least 1 day earlier than in VV-infected DCs and is associated with an accelerated diminution of intracellular levels of Bcl-2 and Bcl-$X_L$. In infected DCs, MVA inhibited cellular protein synthesis more rapidly than VV and induced a distinct pattern of viral protein expression that included enhanced expression of the viral dsRNA-binding protein (E3L). The reported enhanced immunogenicity of MVA in comparison to VV despite the earlier induction of DC apoptosis and more rapid inhibition of protein synthesis (in the context of a similarly abortive infection) demonstrated here is notable and suggests that immunity to MVA-vectored vaccines may develop substantially as a result of cross-presentation.

## MATERIALS AND METHODS

**Human subjects.** Whole blood or leukapheresis samples were obtained from healthy human volunteers. All studies were approved by the Emory University Institutional Review Board.

**Culture media.** The medium used to generate monocyte-derived DCs was RPMI 1640 supplemented with 10 mmol of HEPES/liter; 5 mmol of L-glutamine/liter; 100 μg of penicillin, streptomycin, and amphotericin B (all from Mediatech, Herndon, VA)/ml; and 10% fetal bovine serum (FBS; HyClone, Logan, UT). The medium used to grow the DF-1 and HeLa cell lines was Dulbecco modified Eagle medium (DMEM; Mediatech) supplemented with 10 mmol of HEPES/liter; 5 mmol of L-glutamine/liter; 100 μg of penicillin, streptomycin, and amphotericin B/ml; and 10% FBS. For metabolic labeling, the medium used for DCs was methionine-free RPMI (Mediatech) supplemented with 10 mmol of HEPES/liter; 5 mmol of L-glutamine/liter; 100 μg of penicillin, streptomycin, and amphotericin B/ml; and 10% FBS. The medium used for the cell lines was methionine-free DMEM (Sigma Chemical Co., St. Louis, MO) supplemented with 10 mmol of HEPES/liter; 5 mmol of L-glutamine/liter; 100 μg of penicillin, streptomycin, and amphotericin B/liter; and 2% FBS.

**Mononuclear cell subsets. (i) PBMC.** PBMC were isolated from whole-blood or leukapheresis samples by standard density gradient centrifugation on lymphocyte separation medium (ICN Biomedicals, Aurora, OH). Red blood cells were lysed with ACK lysing buffer (Biosource, Camarillo, CA).

**(ii) DCs.** DCs were obtained by one of two methods. (i) Monocytes were selected from PBMC by using an anti-CD14 monoclonal antibody (MAb) conjugated to magnetic beads (Miltenyi Biotec, Auburn, CA), and $2.5 \times 10^6$ monocytes were plated in 3 ml of RPMI–10% FBS/well in six-well plates. (ii) A total of $10 \times 10^6$ to $15 \times 10^6$ PBMC were incubated for 2 h at 37°C in 3 ml of RPMI–10% FBS/well in six-well plates to allow monocytes to adhere, washed with phosphate-buffered saline (PBS; Mediatech), and then cultured in 3 ml of RPMI–10% FBS/well. For each method, cultures were fed with 1,000 IU of recombinant human granulocyte-macrophage colony-stimulating factor (Peprotech, Rocky Hill, NJ)/ml and 725 IU of recombinant human interleukin-4 (R&D Systems, Minneapolis, MN)/ml on days 0, 2, 4, and 6, and immature DCs were collected on day 7. Mature DCs were generated by adding 1 μg of lipopolysaccharide (LPS)/ml (Sigma) on day 7 for 24 to 48 h. Immature and mature DC phenotypes were determined by MAb staining and analyzed by flow cytometry.

**Viruses. (i) Virus stocks.** rVV-EGFP (NYCBH strain) expressing enhanced green fluorescent protein (EGFP) under the control of the p7.5 early-late promoter was a gift from L. Corey (University of Washington). rMVA-GFP was constructed to contain a recombinant GFP-ZEO fusion protein that expresses GFP under the control of the early H5 promoter and that confers resistance to zeocin (Invitrogen, Carlsbad, CA). rVV stocks were expanded in HeLa cells (American Type Culture Collection [ATCC], Manassas, VA), and titers were determined on BSC40 cells (ATCC). rMVA stocks were expanded in the chicken embryo fibroblast cell line DF-1 (ATCC), and titers were determined on DF-1 cell monolayers. Viruses were purified by sucrose gradient sedimentation, and titers were determined by serial dilutions and plaque assays. For all viruses, both intracellular and extracellular particles were collected. However, stocks were subjected to at least one freeze-thaw cycle, which results in disruption of the outer membrane of extracellular enveloped virions (34).

**(ii) Virus infection.** Cells were infected with rVV-EGFP or rMVA-GFP at a multiplicity of infection (MOI) of 10 or 1 (as indicated) for 1 h at 37°C, washed with either RPMI–10% FBS or DMEM–10% FBS depending on the cell type, and then incubated in RPMI–10% FBS or DMEM–10% FBS in six-well plates at 37°C.

**Antibody staining and flow cytometry.** The following MAbs were purchased from BD Biosciences Pharmingen (San Diego, CA): fluorescein isothiocyanate-, phycoerythrin-, PerCP-, CyChrome-, or APC-conjugated mouse anti-human CD80, CD83, CD86, Bcl-2, Bcl-$X_L$, and appropriate isotype control MAbs. The following MAbs were purchased from BD Biosciences Immunocytometry Systems (San Jose, CA): fluorescein isothiocyanate-, phycoerythrin-, PerCP-, or APC-conjugated mouse anti-human CD11c, CD14, CD25, HLA-DR, and appropriate isotype control MAbs. The MAb A56R (VV1-4G9) was kindly provided by A. Schmaljohn (National Institutes of Health). Samples were acquired on a FACSCalibur flow cytometer (BD Biosciences Immunocytometry Systems) and analyzed by using FlowJo software (TreeStar, San Carlos, CA).

**Vaccinia virus UDG real-time PCR.** Cells were frozen at −80°C at 0, 1.5, 4, and 24 h after infection. DNA was extracted by using the MagNA Pure LC DNA isolation kit I (Roche, Indianapolis, IN) and was quantified by UV spectrometry. The probe and primers for real-time PCR were designed by the use of Primer Express software (Applied Biosystems, Foster City, CA) within the conserved uracil DNA glycosylase (UDG; encoded by *D4R*) region. The TaqMan Probe (5′-CGAGACGAGACGTCGCCTATTCCTG-3′; Applied Biosystems) was labeled at the 5′ end with the reporter dye FAM (6-carboxy-fluorescein) and at the 3′ end with the quencher dye TAMRA (6-carboxyl-tetramethyl-rhodamine) with a melting temperature ($T_m$) of 68°C. The primer sequences were 5′-GGTAGAGTTTTATAACGAAGTAGCCAGTT-3′ (sense; length, 29 bases; $T_m$ = 58°C) and 5′-CTCGTTTATTTCTAAGCGGTTGTTT-3′ (antisense; length, 25 bases; $T_m$ = 58°C). Real-time PCR was performed by using the ABI Prism 7700HT sequence detection system (Applied Biosystems) with TaqMan Gold kit under the following conditions. The 50-μl reactions contained 5 μl of 10× TaqMan buffer A, 4 mM $MgCl_2$, 200 μM deoxynucleoside triphosphates, a 200 nM concentrations of each primer, a 125 nM concentration of the fluorogenic probe, and 1.25 U of AmpliTaq Gold DNA polymerase. Universal thermal cycling conditions consisted of 10 min at 95°C, followed by 45 cycles of 15 s at 95°C and 1 min at 60°C. A total of 200 ng of DNA was analyzed as a template for amplification, and the results obtained were expressed in UDG copies per 200 ng of DNA. Each reaction was carried out in duplicate.

**Immunofluorescence staining.** For immunofluorescence analysis, cells were fixed in 2% formaldehyde and permeabilized in Triton X-100 as described previously (36). Cell nuclei and viral replication centers were recognized by staining with DAPI (4′,6′-diamidino-2-phenylindole; 1 μg/ml; Sigma), and actin was recognized by staining with 546-phalloidin (1 μg/ml; Molecular Probes, Eugene, OR). The MAb directed against A36R (kindly provided by G. Smith, Imperial College of London) was used at 1:200, followed by a donkey anti-mouse secondary antibody (Jackson Immunoresearch, West Grove, PA).

**Microscopy.** Images were acquired with a scientific-grade cooled charge-coupled device (Cool-Snap HQ) on a multiwavelength wide-field three-dimensional microscopy system (Intelligent Imaging Innovations, Baltimore, MD) based on a 200M inverted microscope using a ×63 N.A.1.4 lens (Carl Zeiss, Inc., Thornwood, NJ). Immunofluorescent samples were imaged at room temperature by using a standard Sedat filter set (Chroma Technology Corp., Rockingham, VT) in successive 0.20-μm focal planes through the samples, and out-of-focus light was removed with a constrained iterative deconvolution algorithm (68).

**VV progeny titration.** Cells were frozen at −80°C at 0, 1.5, 12, and 24 h postinfection. Repetitive freeze-thaw cycles were used to lyse the cells, followed by sonication for 1 min. Titers of the supernatant dilutions were determined on BSC40 monolayers for 48 h, and plaques were stained with 0.04% neutral red (Sigma).

**Metabolic labeling of infected cell proteins.** Infected DCs were washed once with cold methionine-free RPMI and then incubated for 30 min (prior to the indicated time points) at 37°C with methionine-free medium supplemented with 30 μCi of $^{35}$S-Translabel (ICN Biomedicals) per million cells. Infected HeLa and DF-1 cells were washed once with cold methionine-free DMEM and then incubated for 30 min (prior to the indicated time points) at 37°C with methionine-free medium supplemented with 60 μCi of $^{35}$S-Translabel per million cells. After labeling, cells were washed once with ice-cold PBS prior to lysis and resolution of proteins via sodium dodecyl sulfate-polyacrylamide gel electrophoresis (SDS-PAGE). Labeled proteins were visualized via autoradiography.

**Proteomic analyses.** DCs were mock infected for 0 or 8 h or were infected with rMVA or rVV for 8 h in triplicate. Proteins were extracted in 8 M urea–4% CHAPS {3-[(3-cholamidopropyl)-dimethylammonio]-1-propanesulfonate}–15 mM Tris (pH 8.4) at 4°C with sonication. Insoluble material was removed by centrifugation at 100,000 × *g* for 4 h at 20°C. Ionic interfering substances were removed, and protein extracts were concentrated with three buffer exchanges of the extraction buffer by using Microcon YM-10 centrifugal filter devices (Millipore, Billerica, MA). A pooled reference sample was created by combining 25 μg of each sample, and all samples were diluted to 5 mg/ml by using the extraction buffer. Then, 50 μg of each individual sample was labeled with 200 pmol of minimal Cy3 or Cy5 NHS ester (GE Healthcare, Little Chalfont, United Kingdom), and the pooled reference sample was labeled in bulk with minimal Cy2 NHS ester (at a ratio of 200 pmol of dye to 50 μg of sample) at 4°C for 30 min. The labeling reaction was quenched with 10 nmol of lysine. Labeled protein extracts were combined, and proteins were separated on 18-cm pH 3-10 IPG strips for 32,000 V · h using an IPGphor (GE Healthcare) in 8 M urea–2% CHAPS–0.5% IPG buffer–18.2 mM dithiothreitol (DTT) and 0.002% bromophenol blue using active rehydration at 30 V. After isoelectric focusing, IPG strips were equilibrated in 6 M urea, 2% SDS, 65 mM DTT, 30% glycerol, 50 mM Tris (pH 8.8), and 0.002% bromophenol blue for 15 min at room temperature. The IPG strips were then equilibrated with the buffer described above, replacing DTT with 135 mM iodoacetamide, for 15 min at room temperature. Proteins were then separated on 20-by-26-cm 8 to 15% SDS-polyacrylamide gels by using Dalt II (GE Healthcare). Gels were fixed in 30% ethanol and 7.5% acetic acid overnight at room temperature. Gels were imaged by using the Typhoon 9400 (GE Healthcare), optimizing the photomultiplier tube voltages for each laser to achieve the broadest dynamic range and analyzed for significant differences by analysis of variance based on the $\log_2$ standardized volume using DeCyder 4.0 software (GE Healthcare). Gels selected for picking were stained with Sypro Ruby (Molecular Probes) overnight, destained in 10% methanol and 6% acetic acid for 30 min at room temperature, imaged, and matched to the Cy images by using DeCyder software. The pick list was created based on the Sypro image. Gel plugs (2.0 mm) were picked, washed, reduced, alkylated, and digested with trypsin, and the resulting peptides were extracted and spotted by using the spot handling workstation (GE Healthcare). Briefly, the plugs were washed twice with 50 mM ammonium bicarbonate–50% methanol for 20 min at room temperature. Plugs were washed with 75% acetonitrile for 20 min at room temperature and dried at 40°C for 10 min. Plugs were incubated in 10 mM DTT–20 mM ammonium bicarbonate at 37°C for 1 h. The DTT solution was removed and immediately replaced with 100 mM iodoacetamide–20 mM ammonium bicarbonate and incubated at room temperature in the dark for 30 min. The plugs were washed as described above and then incubated with 200 ng of sequencing grade trypsin (Promega, Madison, WI) at 37°C for 2 h. Peptides were extracted twice with 50% acetonitrile–0.1% trifluoroacetic acid for 20 min at room temperature and concentrated by using a SpeedVac (Thermo Electron Corp., Waltham, MA). Approximately 25% of the resulting peptides were spotted with partially saturated α-cyano-4-hydroxy-cinnamic acid (Sigma). Mass spectrometry (MS) and tandem MS (MS/MS) data were acquired by using the 4700 Proteomics Analyzer (Applied Biosystems) by using standard acquisition methods. MS spectra were calibrated by using two trypsin autolysis peaks (1,045.45 and 2,211.096 *m/z*). MS/MS spectra were calibrated by using the instrument default processing method. Mass lists were submitted to subdatabases of NCBInr (*Homo sapiens* and viruses) using Mascot v.1.9.05 (http://www.matrixscience.com/cgi/index.pl?page = /search_form_select.html) and PROWL (http://prowl.rockefeller.edu/), considering fixed cysteine carbamidomethylation and partial methionine oxidation modifications, one missed tryptic cleavage, and 10 ppm mass accuracy. A deduced amino acid sequence was interpreted from the MS/MS spectra manually, with the aid of data explorer software (Applied Biosystems) and submitted to MSBlast (http://dove.embl-heidelberg.de/Blast2/msblast.html). Identifications were cross-examined by using mass accuracy, molecular weight, and pI.

**Caspase activation.** Caspase activation was detected by two methods: (i) The one-step cellular caspase 3/7 assay was performed as described previously (15). Briefly, DCs were plated in 96-well flat-bottom plates at 5 × $10^4$ cells/well and

then infected or UV treated (8 min in a Stratalinker 1800 [Stratagene, La Jolla, CA]). At each time point, the one-step caspase 3/7 assay buffer (containing the caspase 3/7 substrate DEVD-AMC, whose fluorescence is released by enzymatic cleavage; BIOMOL, Plymouth Meeting, PA) was added for 1 h, and the caspase 3/7 activity was measured by using a Spectra Max Plate Reader with an excitation at 360 nm and an emission at 460 nm. For each group, three wells were incubated with buffer containing the caspase 3/7 substrate DEVD-AMC, and three wells were incubated with substrate-free buffer; the mean of the three substrate-free wells was subtracted from the mean of the three substrate-containing wells. In some cases, the pan-caspase inhibitor Z-VAD-FMK (25 μM; BIOMOL) was added concurrent with virus infection. (ii) A cell-permeable, fluorogenic caspase 3 substrate (PhiPhiLux-R2D2, provided by OncoImmunin, Inc., Gaithersburg, MD) was incubated with DCs for 30 min at 37°C, and caspase-mediated cleavage and the resultant fluorophore release was measured by flow cytometry. PhiPhiLux-R2D2 is detected in the FL4 channel.

## RESULTS

**DCs express VV and MVA early genes.** To determine where the block to VV and MVA replication occurs in DCs, we studied a number of discrete stages of the orthopoxvirus life cycle. We have previously shown that both primary plasmacytoid and myeloid DC subsets express EGFP controlled by an early/late viral promoter after exposure to VV (17). To confirm that viral early genes are expressed in the human monocyte-derived DCs used in the present study, we utilized a recombinant MVA expressing GFP under control of the modified H5 early promoter (rMVA-GFP) and a recombinant VV expressing EGFP under the control of the p7.5 early/late viral promoter (rVV-EGFP). The myeloid lineage monocyte-derived DCs have been used extensively for studies of Ag processing and presentation (10). Representative phenotypes of immature ($CD11c^+$ $CD86^+$ $CD14^-$ $CD80^-$ $CD83^{lo}$ $CD25^-$) and LPS-matured ($CD80^+$ $CD83^{hi}$ $CD25^+$) monocyte-derived DCs are shown in Fig. 1A. Immature and mature DCs were mock infected or infected with rVV-EGFP or rMVA-GFP at an MOI of 10, and the percentage of DCs with increased green fluorescence was monitored by flow cytometry at 0, 6, 12, 24, and 48 h postinfection. Maximal numbers of immature DCs with increased green fluorescence were observed at 12 h after MVA infection (55% $GFP^+$, Fig. 1B) and 24 h after VV infection (72% $EGFP^+$, Fig. 1C). Due to the use of different promoters controlling (E)GFP and the different GFP variants included in these two viruses, a direct comparison of the levels of early gene expression in MVA- versus VV-infected DCs could not be made. Nevertheless, differences in the susceptibility of immature and mature DCs to each virus were seen. rVV-EGFP infection resulted in a greater percentage of immature DCs expressing EGFP compared to mature DCs (at all time points), an observation that is consistent with previous reports (25). In contrast, rMVA-GFP infection resulted in approximately equal percentages of $GFP^+$ immature and mature DCs. Mock-infected DCs displayed no green fluorescence (data not shown).

**DCs support limited VV and no MVA DNA synthesis.** After the expression of early genes, poxviruses uncoat and begin to replicate their DNA. Using a modified dot blot hybridization assay, Drillien et al. reported that DCs fail to replicate VV DNA (23). We sought to extend this finding by analyzing both VV- and MVA-infected DCs and by using methods that allow for the sensitive and quantitative assessment of viral genome copy number and the direct visualization of the virus replication cycle in cells. To determine quantitatively whether DCs support VV or MVA DNA synthesis, we developed a real-time quantitative PCR (Q-PCR) assay to detect the conserved poxvirus UDG (encoded by VV *D4R*/MVA 101R) gene. DCs were infected with rMVA-GFP or rVV-EGFP at an MOI of 10 or 1 and a chicken embryo fibroblast cell line (DF-1) that is permissive for both viruses served as a positive control. After 1.5 h of infection, cells were extensively washed prior to lysis for Q-PCR or replating for later time points; therefore, the UDG

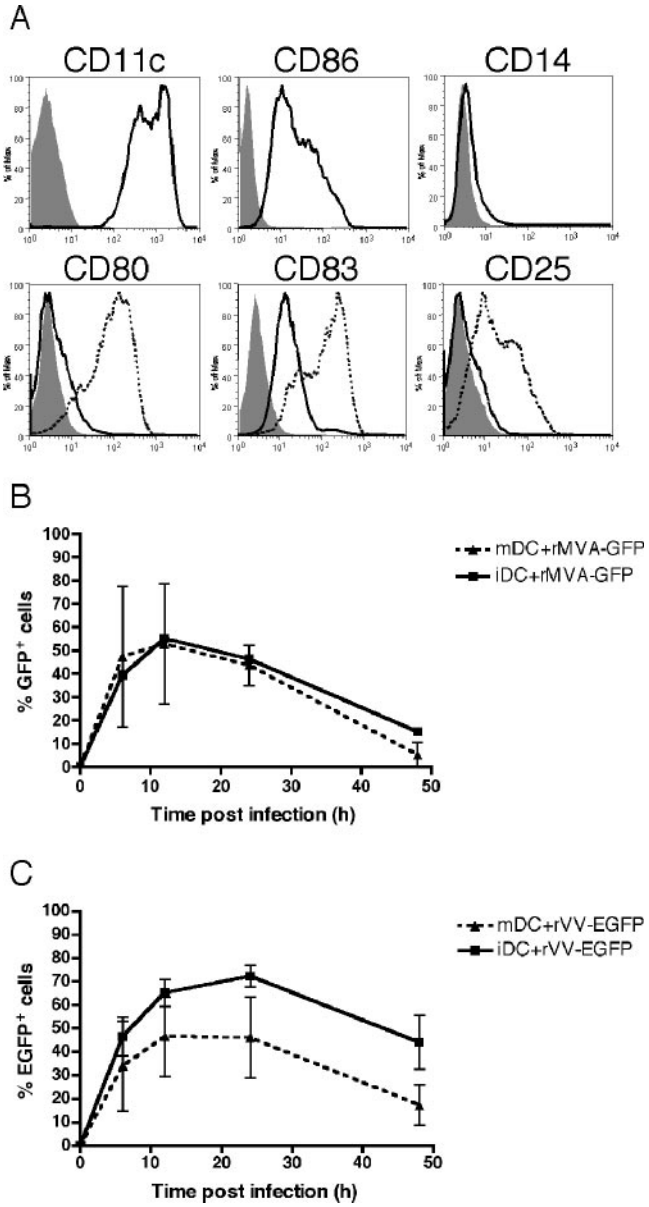


FIG. 1. Infection of immature and mature DCs with VV and MVA and expression of early viral genes. (A) Representative phenotypes of immature (solid histograms) and LPS-matured (dashed histograms) monocyte-derived DCs are shown, as assessed by MAb staining and flow cytometry (filled histograms, isotype controls). Immature or LPS-matured DCs were then infected with rMVA-GFP (B) or rVV-EGFP (C) at an MOI of 10 and (E)GFP expression was measured by flow cytometry at 6, 12, 24, and 48 h. The mean of four donors is shown for immature DCs (iDC) and mature DCs (mDC).

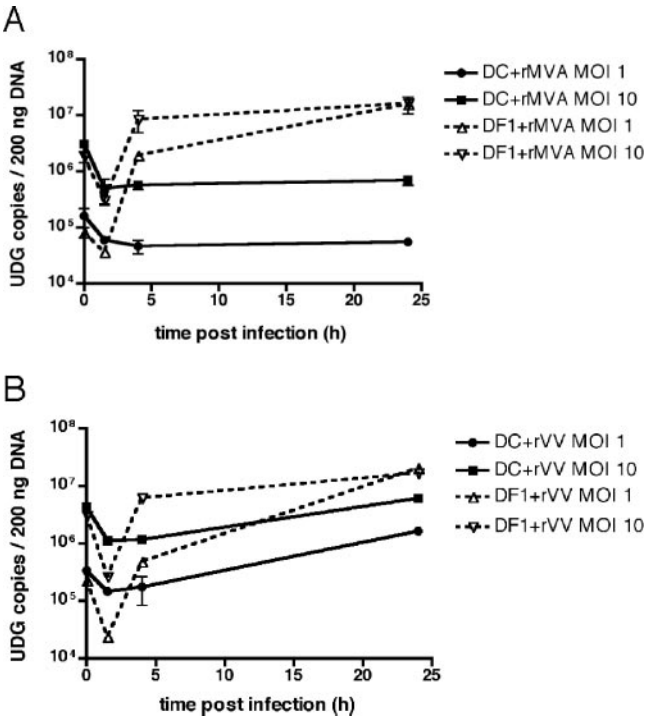


FIG. 2. VV DNA synthesis is limited, and MVA DNA synthesis is absent in DCs. DF- 1 cells and immature DCs were infected in duplicate with rMVA-GFP (A) or rVV-EGFP (B) at an MOI of 1 or 10 for 0, 1.5, 4, and 24 h. At each time point, cells were lysed, total DNA was extracted, and viral replication was assessed by real-time PCR with primers specific for the poxvirus UDG gene. The datum points indicate replicates for each time point, with lines drawn to fit the mean.

copy number at 1.5 h represents viruses that have entered the cell (and does not include defective or noninfectious virus particles likely quantitated at 0 h) and was used as the input copy number for statistical comparisons. DF-1 cells displayed a significant increase in UDG copy number after 24 h of infection with MVA (430- and 53-fold for MOIs of 1 and 10, respectively [$P < 0.001$]; Fig. 2A) or VV (865- and 63-fold for MOIs of 1 and 10, respectively [$P < 0.001$]; Fig. 2B). In contrast, MVA did not demonstrate any increased UDG DNA synthesis in DCs (Fig. 2A), and a limited increase in UDG copy number was seen in DCs infected with VV at an MOI of 1, but not at an MOI of 10, after 24 h (5-fold [$P < 0.01$]; Fig. 2B). Thus, VV shows very limited DNA replication in DCs and, in contrast to reports of a later block in other nonavian cells (28, 60, 67), MVA aborts prior to DNA synthesis in DCs.

**Viral replication centers are not formed in VV- or MVA-infected DCs.** To visualize the block to viral DNA synthesis in DCs, we next assessed the formation of juxtanuclear replication centers by indirect immunofluorescence and wide-field deconvolution microscopy. DCs (Fig. 3G to R and W to Z) or DF-1 cells (Fig. 3A to F and S to V) were adhered to Alcian-blue coated glass coverslips and infected with either rVV-EGFP (Fig. 3A to L) or rMVA-GFP (Fig. 3S to Z) at an MOI of 10 for 8 h. Infected cells were identified by their green fluorescence, indicating (E)GFP expression (Fig. 3B, H, T, and X). An uninfected DC is shown in Fig. 3M to R. Cell nuclei and cytoplasmic viral replication centers were identified by DAPI staining. The juxtanuclear viral replication centers were present in DF-1 cells infected by VV (Fig. 3A) and MVA (Fig. 3S) but were not present in DCs infected by VV (Fig. 3G) or MVA (Fig. 3W). Fifty (E)GFP$^+$ DCs were counted per slide, and no extranuclear DAPI staining was observed. Further, viral replication centers were also not present in DCs after 24 h of VV or MVA infection (data not shown), indicating that orthopoxvirus infection of DCs is not merely slowed down in comparison to permissive cell lines. These data show that, although a small amount of DNA replication may occur after VV infection of DCs (Fig. 2B), the newly synthesized viral DNA is of such a low level as to be undetectable by immunofluorescence and that DCs do not support the formation of VV replication centers. In addition, both viral DNA synthesis and replication center formation are completely blocked in MVA-infected DCs.

**DCs do not express VV or MVA late genes or form actin tails.** The orthopoxvirus life cycle is sequential, with each step requiring completion of the previous one. To determine whether the block to DNA replication inhibits further stages in the life cycle of VV and MVA, we looked for late gene expression and the consequent polymerization of actin in infected DCs. Actin polymerization results in the formation of actin tails that propel new virus particles toward apposing cells. This event is dependent on tyrosine kinase-mediated phosphorylation of the product of the viral gene *A36R* (27) that accumulates late in infection (56). A36R protein is present on the IEV outer membrane and gets deposited on the plasma membrane when IEV fuses to become CEV (72).

Cells were infected as described above and, after 8 h, stained with 546-phalloidin to detect actin and an MAb directed against A36R. Actin tails were prominent structures in both VV (Fig. 3C)- and MVA (Fig. 3U)-infected DF-1 cells. In contrast, infected DCs displayed actin staining primarily localized to their dendrites (similar to uninfected DCs; Fig. 3O), but no tails were observed after VV (Fig. 3I) or MVA (Fig. 3Y) infection. We next observed A36R protein in a cytoplasmic location separate from the replication centers (Fig. 3E and F) and on the tips of the actin tails (Fig. 3F and inset) in VV-infected DF-1 cells. VV-infected DCs, by contrast, were negative for A36R staining (Fig. 3K), indicating a lack of the late accumulation of A36R protein and, consequently, of actin polymerization.

MVA-infected DF-1 cells did not stain with the A36R MAb (data not shown). We believe that, compared to the VV allele, the two in-frame deletions in the A36R homolog encoded by MVA (*147R*) may result in a loss of antibody binding to the shorter protein (6), although they do not affect protein function, as evidenced by actin tail formation in MVA-infected DF-1 cells (Fig. 3U). The *A56R* gene, which is intact in MVA, is under the control of early and late promoters, but the majority of encoded hemagglutinin (HA) protein accumulates late (13). Using MAb staining for A56R and flow cytometry, we found that rMVA-GFP-infected DF-1 cells express high levels of HA but that rMVA-GFP-infected DCs do not (at 12, 24, and 48 h postinfection, Fig.3AA); the low level of A56R staining seen in DCs is presumably a result of the minority of HA that is expressed early.

**VV does not produce infectious progeny in DCs.** We have shown that viral replication center formation, late gene expres-

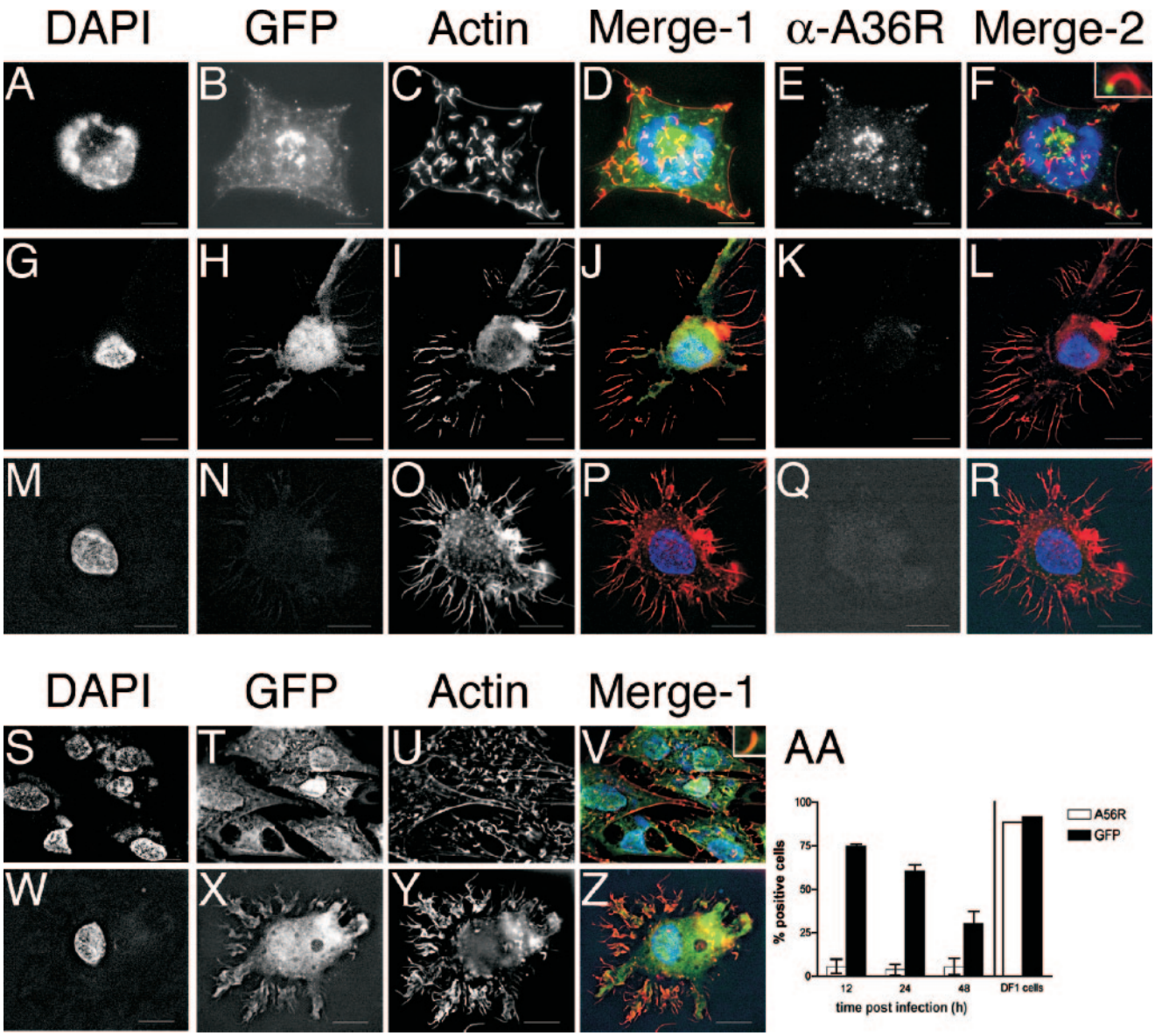


FIG. 3. VV and MVA do not form viral replication centers in DCs. Immature DCs (G to R and W to Z) or DF-1 cells (A to F and S to V) were adhered to Alcian blue-coated glass coverslips and then infected with rVV-EGFP (A to L) or rMVA-GFP (S to Z) at an MOI of 10 for 8 h. DCs were also mock infected (M to R). Cells were stained with DAPI (A, G, M, S, and W) to identify cell nuclei and juxtanuclear viral replication centers, Alexa Fluor 546-phalloidin (C, I, O, U, and Y) to identify actin, and anti-A36R Cy5 (E, K, and Q) to identify viral late gene expression. (E)GFP fluorescence was used to identify infected cells that express viral early genes (B, H, N, T, and X). In the merged images, DAPI is pseudocolored blue, (E)GFP (Merge-1) or A36R (Merge-2) is green, and actin is red. Insets in panels F and V show higher magnification of actin tail. (AA) Immature DCs (left) or DF-1 cells (right) were infected with rMVA-GFP at an MOI of 10 and then stained with an MAb directed against the product of the viral late gene *A56R*. A56R and GFP expression were measured by flow cytometry.

sion, and actin polymerization are blocked in both VV- and MVA-infected DCs. Since we saw limited VV DNA synthesis in DCs by Q-PCR, we wanted to confirm the nonpermissive nature of VV infection of DCs, as reported by others (12, 23, 25, 35, 66). To determine whether VV infectious progeny are made in DCs, we used serial dilutions to titer infected DC lysates on BSC40 cell monolayers and counted the resultant plaques. DCs were infected with rVV-EGFP at an MOI of 10 or 1, and cell lysates were collected at 0, 1.5, 12, and 24 h postinfection. As shown in Fig. 4, the number of input infectious virus particles was $1.5 \times 10^7$ and $2.25 \times 10^6$ for MOIs of 10 and 1, respectively. At subsequent time points a large reduction in plaques (550- and 490-fold for MOIs of 10 and 1, respectively, at 24 h) was seen, indicating that VV infectious progeny were not produced.

**MVA infection results in a distinct pattern of viral protein synthesis and earlier inhibition of host protein synthesis in DCs compared to VV.** Orthopoxviruses induce an inhibition of host macromolecule (DNA, RNA, and protein) synthesis that is believed to favor the production of virus-encoded structural and enzymatic products and virus replication and occurs in response to virion proteins or viral early gene products (8, 14).

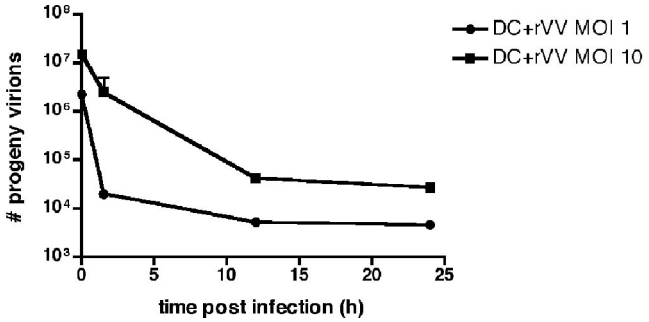


FIG. 4. VV does not make infectious progeny in DCs. Immature DCs were infected with rVV-EGFP at an MOI of 1 or 10, and at 0, 1.5, 12, and 24 h postinfection the cells were lysed and titers of the supernatants were determined on BSC40 monolayers in duplicate. After 2 days, the plates were stained with neutral red, and plaques were counted the following day. Titers are presented as PFU per milliliter, and replicates for each time point are shown, with a line drawn to fit the mean.

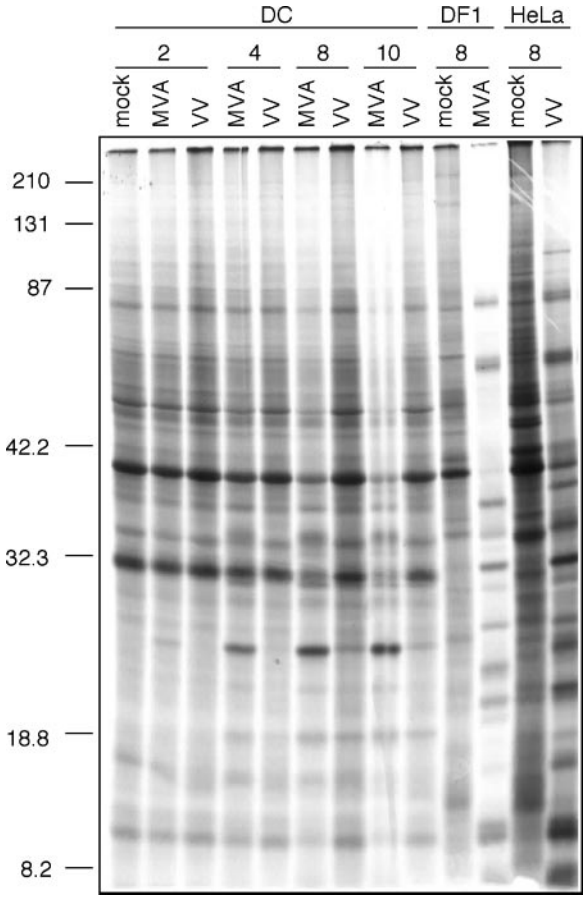


FIG. 5. MVA induces more rapid host protein synthesis inhibition in DCs than VV. Immature DCs were infected with rMVA-GFP or rVV-EGFP, DF-1 cells were infected with rMVA-GFP, and HeLa cells were infected with rVV-EGFP—all at an MOI of 10. Cells were labeled with [$^{35}$S]methionine for 0.5 h at the indicated times postinfection. Virus- and mock-infected cell lysates were then separated by SDS-PAGE, followed by autoradiography. Molecular weight markers are indicated to the left of the gel.

Because virus entry and early gene expression are intact in VV- and MVA-infected DCs, we next investigated the inhibition of host cell protein synthesis as a measure of the virus-induced cytopathic effect. DCs were infected with rMVA-GFP or rVV-EGFP at an MOI of 10, and cell lysates were metabolically labeled with [$^{35}$S]methionine at 2, 4, 8, and 10 h postinfection. The permissive cell lines DF-1 and HeLa were infected with rMVA-GFP and rVV-EGFP, respectively, and labeled at 8 h postinfection for comparison. Inhibition of protein synthesis in MVA-infected DCs began at 4 h postinfection, and protein levels further decreased over time (Fig. 5). In VV-infected DCs, in contrast, a less pronounced inhibition of protein synthesis was observed beginning at 10 h postinfection (Fig. 5). As expected, each of the cell lines demonstrated a substantial shutoff of cellular protein synthesis at 8 h postinfection, with a shift toward the characteristic pattern of viral late protein expression (Fig. 5).

Surprisingly, despite the progressive inhibition of protein synthesis that occurs in MVA-infected DCs, synthesis of a small number of new proteins in a pattern distinct from that of the permissive cell lines was observed after MVA and, to a lesser extent, VV infection. In particular, synthesis of a single prominent new protein (~25 kDa) was observed as early as 2 h postinfection in MVA-infected DCs, with increased expression over the following 8 h (Fig. 5). This protein band was not detectable through 8 h postinfection in VV-infected DCs but was eventually observed at a much lower level after 10 h. To identify this differentially expressed protein, proteomic analysis of MVA and VV-infected DCs was performed. In these studies, DCs were mock infected or were infected with rMVA or rVV for 8 h, followed by cell lysis, and isolated proteins were analyzed by two-dimensional gel electrophoresis. A protein of 20 to 25 kDa (pI = 5.0 to 5.5) was identified to be specifically expressed in MVA-infected DCs and was isolated for subsequent proteomic analysis via tryptic digestion and matrix-assisted laser desorption ionization–time of flight MS analysis as described previously (see Materials and Methods). This differentially expressed protein was identified as the poxvirus dsRNA binding protein (MVA 050L/VV E3L) based on a concordance of results from peptide mass fingerprint analysis (4 matched peptides/24 measured peptides, 27% minimum sequence coverage) and tandem MS identification of a tryptic peptide LLGYV(L/I)(L/I)RF ($m/z$ = 1,093) that corresponds to amino acids 182 to 190 (LLGYVIIRF) of the MVA 050L gene product (data not shown).

**MVA induces earlier apoptosis in DCs compared to VV.** Both VV and MVA have been reported to induce the apoptosis of infected DCs (25, 66, 71), but measurements of apoptotic cell death prior to 24 h postinfection have not been performed and, as such, no information as to the kinetics and mechanism of apoptosis induction exists. Since both MVA and VV complete their life cycles in permissive cells in less than 8 h (D. Kalman, unpublished observations), studies conducted earlier in infection may be particularly relevant. We wondered whether the early shutoff of host protein synthesis, particularly after MVA infection, would lead to rapid DC apoptosis and whether this apoptosis was the cause of the early block to viral replication. To compare the timing of apoptosis induction in

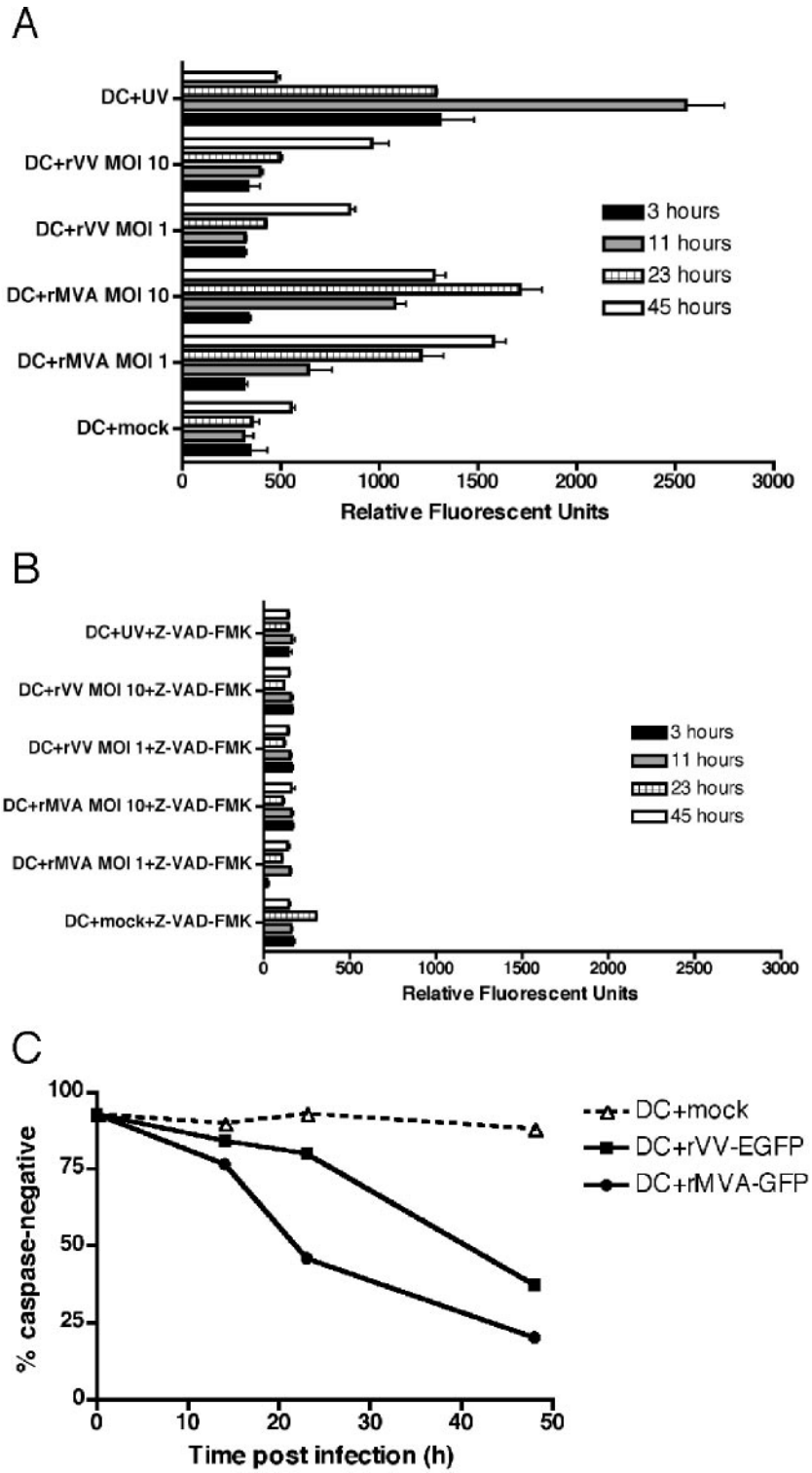


FIG. 6. MVA induces earlier caspase activation in DCs than VV. (A) Immature DCs were mock treated, infected with rMVA-GFP or rVV-EGFP at an MOI of 1 or 10, or UV treated. Apoptosis was measured at 3, 11, 23, and 45 h by one-step cellular caspase 3/7 assay. (B) The same experiment was performed as in panel A, with the addition of the pan-caspase inhibitor Z-VAD-FMK to demonstrate the specificity of the assay. (C) Immature DCs were either mock infected (dashed line, triangles) or were infected with rVV-EGFP (solid line, squares) or rMVA-GFP (solid line, circles) at an MOI of 10. Apoptosis was measured at 0, 14, 23, and 48 h postinfection by flow cytometry after staining of the cells with the fluorogenic caspase substrate R2D2. These data are representative of results from four independent experiments.

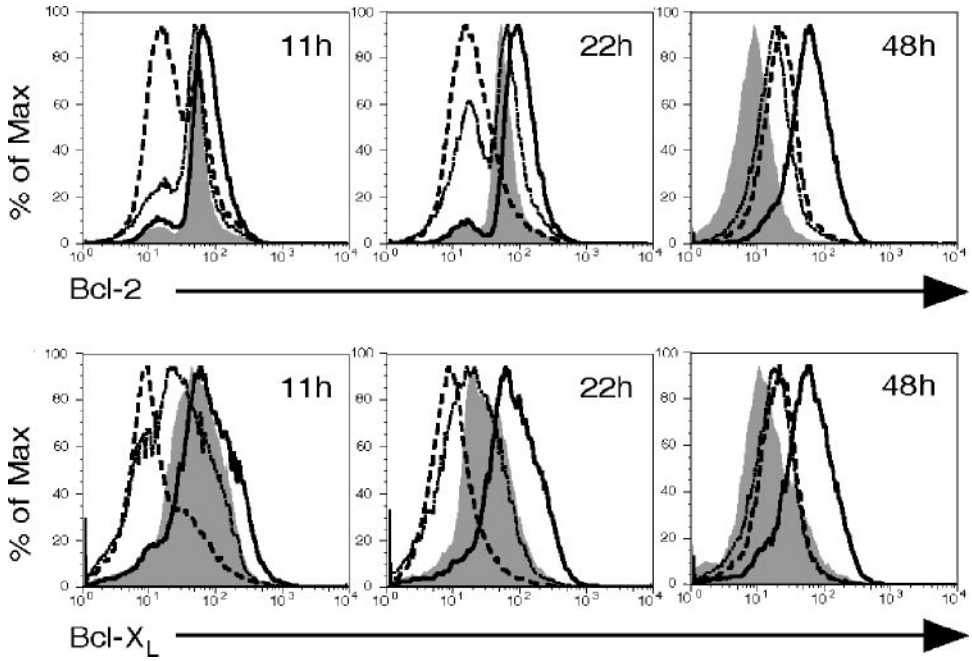


FIG. 7. MVA induces earlier downregulation of Bcl-2 and Bcl-$X_L$ expression in DCs than VV. Immature DCs were mock treated (shaded histogram), infected with rVV-EGFP (dotted histogram) or rMVA-GFP (dashed histogram) at an MOI of 10, or treated with LPS (1 μg/ml, solid histogram), and the intracellular levels of Bcl-2 and Bcl-$X_L$ were measured by using MAb staining and flow cytometry at 11, 22, and 48 h postinfection. These data are representative of results from three independent experiments.

MVA- versus VV-infected DCs, we measured intracellular caspase activation with fluorogenic substrates for the effector caspases 3 and 7 (15). We chose caspase activation specifically because it is a relatively early and physiologically relevant indicator of apoptotic cell death and because different apoptotic pathways converge at the point of effector caspase activation (43). DCs were mock infected, infected with rMVA-GFP or rVV-EGFP at an MOI of 10 or 1, or UV irradiated, and caspase 3/7 activation was monitored at 3, 11, 23, and 45 h postinfection. As shown in Fig. 6A, the UV-treated cells exhibited high levels of caspase 3/7 activation at all time points except 45 h (at which point the cells had completely disassembled). At both MOIs, MVA-infected DCs displayed sustained caspase 3/7 activity above mock-infected cells beginning at 11 h postinfection, whereas VV-infected DCs only showed caspase 3/7 activation at the 45 h time point. The pan-caspase inhibitor Z-VAD-FMK was used to demonstrate the assay's specificity for caspase activity (Fig. 6B).

Since the caspase 3/7 activation assay described above did not allow us to quantify the percentage of viable cells at each time point, we next repeated the virus infections and monitored caspase activation in DCs at the single cell level by flow cytometry with a fluorogenic caspase 3 substrate (39, 43). By this measure, rMVA-GFP-infected DCs displayed caspase 3 activity above that of mock-infected controls after 14 h of infection, with increasing numbers of caspase-positive cells seen after 23 and 48 h (Fig. 6C). The majority of rVV-EGFP-infected DCs first demonstrated caspase 3 activity after 48 h of infection, at which point 63% of the VV-infected DCs and 80% of the MVA-infected DCs were apoptotic (Fig. 6C). Thus, by both measures of caspase activation, we consistently find that DCs exposed to MVA initiate apoptosis at least 1 day earlier than DCs exposed to VV.

**MVA induces earlier Bcl-2 and Bcl-$X_L$ downregulation in DCs compared to VV.** The mitochondrial pathway of apoptosis is regulated by pro- and antiapoptotic members of the Bcl-2 family of proteins (2). We hypothesized that the more rapid apoptosis observed after MVA infection may, in part, be due to alterations in the levels of these proteins. To determine whether orthopoxvirus infection induces a downregulation of host antiapoptotic factors (perhaps influenced by the general block to host protein synthesis), DCs were mock infected, infected with rVV-EGFP or rMVA-GFP at an MOI of 10, or treated with LPS (1 μg/ml), and intracellular expression of Bcl-2 and Bcl-$X_L$ was monitored by flow cytometry at 11, 22, and 48 h postinfection. LPS-treated (i.e., mature) DCs displayed increased levels of Bcl-2 and Bcl-$X_L$ compared to mock-infected cells at all time points (Fig. 7 and Table 1), as has been observed by others (45). Immature DCs are not long-lived in culture; accordingly, at 48 h, mock-infected cells downregulated Bcl-2 and Bcl-$X_L$ expression (Fig. 7 and Table 1), indicating a lower threshold for activation of the mitochondrial pathway of apoptosis. Significantly, MVA induced a greater and earlier decrease in the levels of Bcl-2 and Bcl-$X_L$ compared to VV, with downregulation of both proteins already apparent at 11 h postinfection (Fig. 7 and Table 1). By 48 h, the levels of Bcl-2 and Bcl-$X_L$ in VV- or MVA-infected DCs were similar (Fig. 7 and Table 1). These results suggest that MVA triggers earlier effector caspase activation as a result of mitochondrial depolarization caused by cellular antiapoptotic factor downregulation combined with a compromised ability to synthesize new antiapoptotic proteins.

TABLE 1. Mean fluorescence intensity of Bcl-2 and Bcl-$X_L$[a]

| DC group | MFI | | | | | |
|---|---|---|---|---|---|---|
| | Bcl-2 | | | Bcl-$X_L$ | | |
| | 11 h p.i. | 22 h p.i. | 48 h p.i. | 11 h p.i. | 22 h p.i. | 48 h p.i. |
| DC + mack | 60 | 63 | 11 | 77 | 48 | 26 |
| DC + rMVA-GFP | 39 | 30 | 26 | 31 | 17 | 29 |
| DC + rVV-EGFP | 50 | 56 | 21 | 52 | 35 | 28 |
| DC + LPS | 82 | 108 | 73 | 114 | 113 | 78 |

[a] MFI, mean fluorescence intensity; p.i., postinfection.

## DISCUSSION

DCs play a pivotal role in both innate and adaptive immune responses. Immature DCs that encounter Ag in the periphery travel to the lymph nodes, maturing en route, and activate Ag-specific $CD4^+$ and $CD8^+$ T cells (10). In the case of viruses that infect DCs, it is crucial to investigate the consequences of infection to obtain a better understanding of the mechanisms by which immunity is generated. For orthopoxvirus-based vaccine candidates, such as MVA, studies of their interactions with DCs will likely suggest ways in which these constructs can be optimized (i.e., by the deletion or insertion of genes with specific immunomodulatory functions) for increased immunogenicity. In earlier investigations of the cellular tropism of orthopoxviruses, we have shown that VV and MVA preferentially target both human DCs (myeloid [$CD11c^+$] and plasmacytoid [$CD123^+$] subsets) and murine DCs for infection (17; Liu et al., unpublished). In the present study, we sought to further characterize the infection of human DCs with VV and MVA and specifically to examine the virus-induced cytopathic effect and virus replication cycle in DCs. We demonstrate that, in contrast to the late block seen in other nonavian cells, MVA aborts early in its life cycle (prior to the formation of viral replication centers) in infected human DCs and confirm that VV is similarly blocked in this cell type. Both abortive infections result in apoptosis of DCs, but we show that DCs exposed to MVA die significantly earlier than those exposed to VV. In comparison to VV-infected DCs, the accelerated apoptosis of MVA-infected DCs is associated with a more rapid diminution of Bcl-2 and Bcl-$X_L$ levels that is likely related to MVA's prompt inhibition of global protein synthesis.

The block to viral DNA synthesis that we describe in VV- and MVA-infected DCs has been observed in other types of VV-infected APCs, including primary human macrophages (11) and WEHI-231, an immature murine B-cell lymphoma (9). In addition, we have found that primary human B cells infected with VV or MVA do not express viral late proteins (17). Taken together, these data suggest that there may be a common response of APCs to orthopoxvirus infection. In fact, unlike non-APCs that typically demonstrate cell lysis as a consequence of the virus cytopathic effect (58), macrophages and B cells, like DCs, undergo apoptosis after VV infection, and this apoptosis is associated with decreased expression of Bcl-$X_L$ and Bcl-2, respectively (9, 33). We have shown here for the first time that members of the Bcl-2 family of proteins are also implicated in DC apoptosis after MVA and, to a lesser extent, VV infection. The different kinetics of apoptosis induction seen after DC infection with VV versus MVA may be due in part to the absence in MVA of certain antiapoptotic proteins (such as SPI-2 encoded by *B13R*) or other as-yet-uncharacterized molecules. The role of the mitochondrial pathway of apoptosis after orthopoxvirus infection is further emphasized by the recent discovery of the VV/MVA-encoded F1L protein that localizes to the mitochondria, interferes with activation of the proapoptotic protein Bak, and prevents the release of cytochrome *c* (26, 73, 74). Due to the expression of F1L and other virus-encoded antiapoptotic proteins (e.g., the *E3L* gene product), the induction of apoptosis after orthopoxvirus infection is relatively uncommon in non-APC cell types (58), indicating further that APCs (including DCs, macrophages, and B cells) may respond to infection via a shared pathway. In this regard, we have observed early and high-level synthesis of the poxvirus dsRNA binding protein (encoded by MVA *050L*/VV *E3L*) during infection of DCs with MVA. While the overall significance of this observation is unclear at present, the increased expression in MVA-infected DCs (that undergo apoptosis more rapidly than do VV-infected DCs) of E3L, a viral factor that exhibits antiapoptotic activity in non-APC cell types (42), illustrates differences in this gene's transcription, translation, and/or protein stability in MVA-versus VV-infected DCs. It remains to be determined what impact this may have on host cell physiology or vector immunogenicity, but it highlights the importance of using primary human cells (in contrast to transformed cell lines) for immunologic studies of poxvirus infections.

The specific trigger for DC apoptosis must be present early in the virus replication cycle and may involve an interaction at the virus-cell surface interface, a component of the internalized virion (58), or a viral early gene product (33). In response to this trigger, DCs and other APCs activate cell signaling pathways that result in reduced expression of cellular antiapoptotic factors (e.g., Bcl-2 and Bcl-$X_L$) and that lead to their apoptosis despite the expected presence of virus-encoded antiapoptotic proteins. The shutoff of host protein synthesis, known to be induced by virion proteins or viral early gene products (8, 14), may significantly impact the induction of apoptosis (and the timing of that induction) since DCs would be prevented from synthesizing antiapoptotic proteins de novo to compensate for the downregulation of Bcl-2 and Bcl-$X_L$. The induction of apoptosis in cells, such as APCs, that only express viral early genes may also be related to the loss of protective viral protein(s) expressed late. Although most viral late genes encode structural proteins, evidence for this hypothesis comes from studies of an rMVA mutant that harbors deletion of the viral UDG (*101R*) gene. Unlike wild-type MVA, the virus with UDG deleted does not replicate its DNA in (otherwise) permissive DF-1 cells, does not express viral late genes, and, in fact, induces apoptosis (D. Garber, unpublished data). It may be that, to gain time to replicate in permissive cells, VV and MVA express both early and late antiapoptotic factors, thereby circumventing a host-mediated proapoptotic response to viral infection. The hypothetical late protective factor(s) would not be expressed in the abortively infected DCs, perhaps tipping the balance toward apoptosis.

The association between apoptosis and a block to viral DNA synthesis, as seen in APCs, the above-mentioned MVAΔ*UDG*-

infected DF-1 cells, and VVΔ*E3L*-infected HeLa cells (38), is intriguing. These results may be interpreted as indicating that the induction of apoptosis leads to an abortive infection. In fact, we find a significant temporal delay between the viral life cycle block and the appearance of apoptosis in DCs (this is particularly true with regard to VV infection). In addition, transfecting human Bcl-2 into the murine B-cell line WEHI-231 prevents VV-induced apoptosis but does not allow for a productive infection (9). It seems likely, then, that the block to orthopoxvirus replication in DCs is not the result of the induction of apoptosis but, rather, is caused by an as-yet-unidentified host-virus interaction. In a previous report of VV infection of DCs, it was proposed that, since DCs are terminally differentiated, they may not possess the cellular proteins or nucleotides necessary for orthopoxvirus DNA replication (23). Other data suggest that orthopoxviruses encode all of the enzymes necessary for virus DNA replication (51) and that host proteins are involved only at the level of postreplicative transcription (55). Since other viruses, such as cytomegalovirus, varicella-zoster virus, and measles virus, productively infect DCs (1, 30, 59), it may be that factors other than the terminal differentiation of these cells are responsible for the abortive nature of orthopoxvirus infection.

In light of the significant and durable immune responses observed after infection of mice, monkeys, and humans (18, 24, 29, 31, 57), it is intriguing that MVA and VV both induce apoptosis of the very cells (DCs) that are specialized to initiate antiviral immune responses. Studies of VV Ag presentation in vivo have demonstrated that DCs are the primary activators of T cells in the lymph node and that these DCs disappear by 48 h after infection (53). Norbury et al. attribute this disappearance to the killing of infected cells by antiviral cytotoxic T lymphocytes (CTL) (53). However, since Ag-specific CTL were not detectable until 3 days postinfection, we propose that DCs were lost to virus-induced apoptosis rather than CTL-mediated clearance. Importantly, VV infection inhibits DC maturation and impairs the ability of immature DCs to stimulate T cells in vitro (25, 35). We have found that MVA-infected DCs also do not mature (A. Chahroudi et al., unpublished data), and it should be noted that immature DCs presenting Ag to T cells without the engagement of costimulatory molecules may induce anergy or tolerance (20, 65). Thus, the apoptosis of infected, immature DCs may represent a host strategy to avoid tolerance to viral antigens after orthopoxvirus infection rather than a viral immune evasion strategy to eliminate professional APCs.

Apoptosis of infected DCs and other cells may, in fact, stimulate immunity since uninfected DCs can cross-present exogenous viral antigens acquired from dying cells to $CD8^+$ T cells (3, 41). In addition, uninfected DCs have been shown to endocytose proteosomal intermediates released from live, VV-infected donor cells and to stimulate VV-specific T cells (61). Thus, cross-presentation may be a major mechanism of immune response induction after orthopoxvirus infection. Mature DCs that become infected in vivo may also contribute to the generation of anti-orthopoxviral immunity (via direct presentation), as indicated by in vitro studies (25, 66). Mature DCs are less readily infected with VV than immature DCs, but MVA targets similar numbers of mature and immature DCs (Fig. 1). In addition, mature DCs are more resistant to apoptosis after VV infection (25, 66), perhaps due to the upregulation of Bcl-2 and Bcl-$X_L$ upon DC maturation (Fig. 7). Further studies using viral vectors that are constructed to encode either pro- or antiapoptotic factors may elucidate the role of the virus-induced DC apoptosis in the generation of immunity via direct- or cross-presentation.

In summary, we have identified a number of important consequences of DC infection with the orthopoxviruses VV and MVA. This direct comparison of MVA and VV infection of DCs allowed us to determine that these viruses abort at a similar stage, but that MVA induces its cytopathic effects more rapidly than VV. In addition, we demonstrate the role of anti-apoptotic Bcl-2 family proteins and, by extension, the mitochondria in orthopoxvirus-induced DC apoptosis. Manipulation of the level and kinetics of DC apoptosis after infection may provide a basis for the optimization of MVA-vectored vaccines.

## ACKNOWLEDGMENTS

We thank Lawrence Corey for rVV-EGFP, Beverly Packard for PhiPhiLux-R2D2, and Alan Schmaljohn and Geoffrey Smith for the MAbs to A56R and A36R, respectively. We are grateful to Tracy Andacht for help with proteomic analysis and Guido Silvestri for critical review of the manuscript.

This study was supported by grants from the National Institutes of Health (P01-AI46007 and U19-AI061728) and the Elizabeth Glaser Scientist Award from the Pediatric AIDS Foundation (6-98 EGSA), all awarded to M.B.F.

## REFERENCES

1. **Abendroth, A., G. Morrow, A. L. Cunningham, and B. Slobedman.** 2001. Varicella-zoster virus infection of human dendritic cells and transmission to T cells: implications for virus dissemination in the host. J. Virol. **75:**6183–6192.
2. **Adams, J. M., and S. Cory.** 1998. The Bcl-2 protein family: arbiters of cell survival. Science **281:**1322–1326.
3. **Albert, M. L., B. Sauter, and N. Bhardwaj.** 1998. Dendritic cells acquire antigen from apoptotic cells and induce class I-restricted CTLs. Nature **392:**86–89.
4. **Altenburger, W., C. P. Suter, and J. Altenburger.** 1989. Partial deletion of the human host range gene in the attenuated vaccinia virus MVA. Arch. Virol. **105:**15–27.
5. **Amara, R. R., F. Villinger, J. D. Altman, S. L. Lydy, S. P. O'Neil, S. I. Staprans, D. C. Montefiori, Y. Xu, J. G. Herndon, L. S. Wyatt, M. A. Candido, N. L. Kozyr, P. L. Earl, J. M. Smith, H. L. Ma, B. D. Grimm, M. L. Hulsey, J. Miller, H. M. McClure, J. M. McNicholl, B. Moss, and H. L. Robinson.** 2001. Control of a mucosal challenge and prevention of AIDS by a multiprotein DNA/MVA vaccine. Science **292:**69–74.
6. **Antoine, G., F. Scheiflinger, F. Dorner, and F. G. Falkner.** 1998. The complete genomic sequence of the modified vaccinia Ankara strain: comparison with other orthopoxviruses. Virology **244:**365–396.
7. **Aubert, M., and K. R. Jerome.** 2003. Apoptosis prevention as a mechanism of immune evasion. Int. Rev. Immunol. **22:**361–371.
8. **Bablanian, R., S. Scribani, and M. Esteban.** 1993. Amplification of polyadenylated nontranslated small RNA sequences (POLADS) during superinfection correlates with the inhibition of viral and cellular protein synthesis. Cell Mol. Biol. Res. **39:**243–255.
9. **Baixeras, E., A. Cebrian, J. P. Albar, J. Salas, A. C. Martinez, E. Vinuela, and Y. Revilla.** 1998. Vaccinia virus-induced apoptosis in immature B lymphocytes: role of cellular Bcl-2. Virus Res. **58:**107–113.
10. **Banchereau, J., and R. M. Steinman.** 1998. Dendritic cells and the control of immunity. Nature **392:**245–252.
11. **Broder, C. C., P. E. Kennedy, F. Michaels, and E. A. Berger.** 1994. Expression of foreign genes in cultured human primary macrophages using recombinant vaccinia virus vectors. Gene **142:**167–174.
12. **Bronte, V., M. W. Carroll, T. J. Goletz, M. Wang, W. W. Overwijk, F. Marincola, S. A. Rosenberg, B. Moss, and N. P. Restifo.** 1997. Antigen expression by dendritic cells correlates with the therapeutic effectiveness of a model recombinant poxvirus tumor vaccine. Proc. Natl. Acad. Sci. USA **94:**3183–3188.
13. **Brown, C. K., P. C. Turner, and R. W. Moyer.** 1991. Molecular characterization of the vaccinia virus hemagglutinin gene. J. Virol. **65:**3598–3606.
14. **Buendia, B., A. Person-Fernandez, G. Beaud, and J. Madjar.** 1987. Ribo-

somal protein phosphorylation in vivo and in vitro by vaccinia virus. Eur. J. Biochem. **162:**95–103.
15. **Carrasco, R. A., N. B. Stamm, and B. K. Patel.** 2003. One-step cellular caspase-3/7 assay. BioTechniques **34:**1064–1067.
16. **Carroll, M. W., and B. Moss.** 1997. Host range and cytopathogenicity of the highly attenuated MVA strain of vaccinia virus: propagation and generation of recombinant viruses in a nonhuman mammalian cell line. Virology **238:** 198–211.
17. **Chahroudi, A., R. Chavan, N. Kozyr, E. K. Waller, G. Silvestri, and M. B. Feinberg.** 2005. Vaccinia virus tropism for primary hematolymphoid cells is determined by restricted expression of a unique virus receptor. J. Virol. **79:**10397–10407.
18. **Coulibaly, S., P. Bruhl, J. Mayrhofer, K. Schmid, M. Gerencer, and F. G. Falkner.** 2005. The nonreplicating smallpox candidate vaccines defective vaccinia Lister (dVV-L) and modified vaccinia Ankara (MVA) elicit robust longterm protection. Virology **341:**91–101.
19. **Crotty, S., P. Felgner, H. Davies, J. Glidewell, L. Villarreal, and R. Ahmed.** 2003. Cutting edge: long-term B-cell memory in humans after smallpox vaccination. J. Immunol. **171:**4969–4973.
20. **Dhodapkar, M. V., R. M. Steinman, J. Krasovsky, C. Munz, and N. Bhardwaj.** 2001. Antigen-specific inhibition of effector T-cell function in humans after injection of immature dendritic cells. J. Exp. Med. **193:**233–238.
21. **Dobbelstein, M., and T. Shenk.** 1996. Protection against apoptosis by the vaccinia virus SPI-2 (B13R) gene product. J. Virol. **70:**6479–6485.
22. **Drexler, I., E. Antunes, M. Schmitz, T. Wolfel, C. Huber, V. Erfle, P. Rieber, M. Theobald, and G. Sutter.** 1999. Modified vaccinia virus Ankara for delivery of human tyrosinase as melanoma-associated antigen: induction of tyrosinase- and melanoma-specific human leukocyte antigen A*0201-restricted cytotoxic T cells in vitro and in vivo. Cancer Res. **59:**4955–4963.
23. **Drillien, R., D. Spehner, A. Bohbot, and D. Hanau.** 2000. Vaccinia virus-related events and phenotypic changes after infection of dendritic cells derived from human monocytes. Virology **268:**471–481.
24. **Earl, P. L., J. L. Americo, L. S. Wyatt, L. A. Eller, J. C. Whitbeck, G. H. Cohen, R. J. Eisenberg, C. J. Hartmann, D. L. Jackson, D. A. Kulesh, M. J. Martinez, D. M. Miller, E. M. Mucker, J. D. Shamblin, S. H. Zwiers, J. W. Huggins, P. B. Jahrling, and B. Moss.** 2004. Immunogenicity of a highly attenuated MVA smallpox vaccine and protection against monkeypox. Nature **428:**182–185.
25. **Engelmayer, J., M. Larsson, M. Subklewe, A. Chahroudi, W. I. Cox, R. M. Steinman, and N. Bhardwaj.** 1999. Vaccinia virus inhibits the maturation of human dendritic cells: a novel mechanism of immune evasion. J. Immunol. **163:**6762–6768.
26. **Fischer, S. F., H. Ludwig, J. Holzapfel, M. Kvansakul, L. Chen, D. C. Huang, G. Sutter, M. Knese, and G. Hacker.** 2006. Modified vaccinia virus Ankara protein F1L is a novel BH3-domain-binding protein and acts together with the early viral protein E3L to block virus-associated apoptosis. Cell Death Differ. **13:**109–118.
27. **Frischknecht, F., V. Moreau, S. Rottger, S. Gonfloni, I. Reckmann, G. Superti-Furga, and M. Way.** 1999. Actin-based motility of vaccinia virus mimics receptor tyrosine kinase signalling. Nature **401:**926–929.
28. **Gallego-Gomez, J. C., C. Risco, D. Rodriguez, P. Cabezas, S. Guerra, J. L. Carrascosa, and M. Esteban.** 2003. Differences in virus-induced cell morphology and in virus maturation between MVA and other strains (WR, Ankara, and NYCBH) of vaccinia virus in infected human cells. J. Virol. **77:**10606–10622.
29. **Gomez, C. E., D. Rodriguez, J. R. Rodriguez, F. Abaitua, C. Duarte, and M. Esteban.** 2001. Enhanced $CD8^+$ T-cell immune response against a V3 loop multiepitope polypeptide (TAB13) of HIV-1 Env after priming with purified fusion protein and booster with modified vaccinia virus Ankara (MVA-TAB) recombinant: a comparison of humoral and cellular immune responses with the vaccinia virus Western Reserve (WR) vector. Vaccine **20:**961–971.
30. **Grosjean, I., C. Caux, C. Bella, I. Berger, F. Wild, J. Banchereau, and D. Kaiserlian.** 1997. Measles virus infects human dendritic cells and blocks their allostimulatory properties for $CD4^+$ T cells. J. Exp. Med. **186:**801–812.
31. **Hammarlund, E., M. W. Lewis, S. G. Hansen, L. I. Strelow, J. A. Nelson, G. J. Sexton, J. M. Hanifin, and M. K. Slifka.** 2003. Duration of antiviral immunity after smallpox vaccination. Nat. Med. **9:**1131–1137.
32. **Hochstein-Mintzel, V., H. C. Huber, and H. Stickl.** 1972. Virulence and immunogenicity of a modified vaccinia virus (strain MVA). Z Immunitatsforsch Exp. Klin. Immunol. **144:**104–156. (In German [author's transl.].)
33. **Humlova, Z., M. Vokurka, M. Esteban, and Z. Melkova.** 2002. Vaccinia virus induces apoptosis of infected macrophages. J. Gen. Virol. **83:**2821–2832.
34. **Ichihashi, Y.** 1996. Extracellular enveloped vaccinia virus escapes neutralization. Virology **217:**478–485.
35. **Jenne, L., C. Hauser, J. F. Arrighi, J. H. Saurat, and A. W. Hugin.** 2000. Poxvirus as a vector to transduce human dendritic cells for immunotherapy: abortive infection but reduced APC function. Gene Ther. **7:**1575–1583.
36. **Kalman, D., O. D. Weiner, D. L. Goosney, J. W. Sedat, B. B. Finlay, A. Abo, and J. M. Bishop.** 1999. Enteropathogenic *Escherichia coli* acts through WASP and Arp2/3 complex to form actin pedestals. Nat. Cell Biol. **1:**389–391.
37. **Kettle, S., A. Alcami, A. Khanna, R. Ehret, C. Jassoy, and G. L. Smith.** 1997. Vaccinia virus serpin B13R (SPI-2) inhibits interleukin-1beta-converting enzyme and protects virus-infected cells from TNF- and Fas-mediated apoptosis, but does not prevent IL-1beta-induced fever. J. Gen. Virol. **78**(Pt. 3)**:**677–685.
38. **Kibler, K. V., T. Shors, K. B. Perkins, C. C. Zeman, M. P. Banaszak, J. Biesterfeldt, J. O. Langland, and B. L. Jacobs.** 1997. Double-stranded RNA is a trigger for apoptosis in vaccinia virus-infected cells. J. Virol. **71:**1992–2003.
39. **Komoriya, A., B. Z. Packard, M. J. Brown, M. L. Wu, and P. A. Henkart.** 2000. Assessment of caspase activities in intact apoptotic thymocytes using cell-permeable fluorogenic caspase substrates. J. Exp. Med. **191:**1819–1828.
40. **Lanzavecchia, A., and F. Sallusto.** 2004. Lead and follow: the dance of the dendritic cell and T cell. Nat. Immunol. **5:**1201–1202.
41. **Larsson, M., J. F. Fonteneau, S. Somersan, C. Sanders, K. Bickham, E. K. Thomas, K. Mahnke, and N. Bhardwaj.** 2001. Efficiency of cross presentation of vaccinia virus-derived antigens by human dendritic cells. Eur. J. Immunol. **31:**3432–3442.
42. **Lee, S. B., and M. Esteban.** 1994. The interferon-induced double-stranded RNA-activated protein kinase induces apoptosis. Virology **199:**491–496.
43. **Liu, L., A. Chahroudi, G. Silvestri, M. E. Wernett, W. J. Kaiser, J. T. Safrit, A. Komoriya, J. D. Altman, B. Z. Packard, and M. B. Feinberg.** 2002. Visualization and quantification of T cell-mediated cytotoxicity using cell-permeable fluorogenic caspase substrates. Nat. Med. **8:**185–189.
44. Reference deleted.
45. **Lundqvist, A., T. Nagata, R. Kiessling, and P. Pisa.** 2002. Mature dendritic cells are protected from Fas/CD95-mediated apoptosis by upregulation of Bcl-$X_L$. Cancer Immunol. Immunother. **51:**139–144.
46. **Mayr, A., V. Hochstein-Mintzel, and H. Stickl.** 1975. Passage history, properties, and applicability of the attenuated vaccinia virus strain MVA. Infection **3:**6–16. (In German [NIH Library transl.].)
47. **Mayr, A., H. Stickl, H. K. Müller, K. Danner, and H. Singer.** 1978. The smallpox vaccination strain MVA: marker, genetic structure, experience gained with parenteral vaccination and behavior in organisms with debilitated defense mechanism. Zentbl. Bakteriol. Hyg. I Abt. Orig. B **167:**375–390. (In German [NIH Library transl.].)
48. **McConkey, S. J., W. H. Reece, V. S. Moorthy, D. Webster, S. Dunachie, G. Butcher, J. M. Vuola, T. J. Blanchard, P. Gothard, K. Watkins, C. M. Hannan, S. Everaere, K. Brown, K. E. Kester, J. Cummings, J. Williams, D. G. Heppner, A. Pathan, K. Flanagan, N. Arulanantham, M. T. Roberts, M. Roy, G. L. Smith, J. Schneider, T. Peto, R. E. Sinden, S. C. Gilbert, and A. V. Hill.** 2003. Enhanced T-cell immunogenicity of plasmid DNA vaccines boosted by recombinant modified vaccinia virus Ankara in humans. Nat. Med. **9:**729–735.
49. **McShane, H., A. A. Pathan, C. R. Sander, S. M. Keating, S. C. Gilbert, K. Huygen, H. A. Fletcher, and A. V. Hill.** 2004. Recombinant modified vaccinia virus Ankara expressing antigen 85A boosts BCG-primed and naturally acquired anti-mycobacterial immunity in humans. Nat. Med. **10:**1240–1244.
50. **Mellman, I., and R. M. Steinman.** 2001. Dendritic cells: specialized and regulated antigen processing machines. Cell **106:**255–258.
51. **Moss, B.** 2001. *Poxviridae*: the viruses and their replication, p. 2849–2883. *In* D. M. Knipe, P. M. Howley, D. E. Griffin, R. A. Lamb, M. A. Martin, B. Roizman, and S. E. Straus (ed.), Fields virology, 4th ed. Lippincott/The Williams & Wilkins Co., Philadelphia, Pa.
52. **Mwau, M., I. Cebere, J. Sutton, P. Chikoti, N. Winstone, E. G. Wee, T. Beattie, Y. H. Chen, L. Dorrell, H. McShane, C. Schmidt, M. Brooks, S. Patel, J. Roberts, C. Conlon, S. L. Rowland-Jones, J. J. Bwayo, A. J. McMichael, and T. Hanke.** 2004. A human immunodeficiency virus 1 (HIV-1) clade A vaccine in clinical trials: stimulation of HIV-specific T-cell responses by DNA and recombinant modified vaccinia virus Ankara (MVA) vaccines in humans. J. Gen. Virol. **85:**911–919.
53. **Norbury, C. C., D. Malide, J. S. Gibbs, J. R. Bennink, and J. W. Yewdell.** 2002. Visualizing priming of virus-specific $CD8^+$ T cells by infected dendritic cells in vivo. Nat. Immunol. **3:**265–271.
54. **Norbury, C. C., and L. J. Sigal.** 2003. Cross priming or direct priming: is that really the question? Curr. Opin. Immunol. **15:**82–88.
55. **Oh, J., and S. S. Broyles.** 2005. Host cell nuclear proteins are recruited to cytoplasmic vaccinia virus replication complexes. J. Virol. **79:**12852–12860.
56. **Parkinson, J. E., and G. L. Smith.** 1994. Vaccinia virus gene A36R encodes a $M_r$ 43-50K protein on the surface of extracellular enveloped virus. Virology **204:**376–390.
57. **Ramirez, J. C., M. M. Gherardi, and M. Esteban.** 2000. Biology of attenuated modified vaccinia virus Ankara recombinant vector in mice: virus fate and activation of B- and T-cell immune responses in comparison with the Western Reserve strain and advantages as a vaccine. J. Virol. **74:**923–933.
58. **Ramsey-Ewing, A., and B. Moss.** 1998. Apoptosis induced by a post-binding step of vaccinia virus entry into Chinese hamster ovary cells. Virology **242:** 138–149.
59. **Riegler, S., H. Hebart, H. Einsele, P. Brossart, G. Jahn, and C. Sinzger.** 2000. Monocyte-derived dendritic cells are permissive to the complete replicative cycle of human cytomegalovirus. J. Gen. Virol. **81:**393–399.
60. **Sancho, M. C., S. Schleich, G. Griffiths, and J. Krijnse-Locker.** 2002. The block in assembly of modified vaccinia virus Ankara in HeLa cells reveals new insights into vaccinia virus morphogenesis. J. Virol. **76:**8318–8334.

61. **Serna, A., M. C. Ramirez, A. Soukhanova, and L. J. Sigal.** 2003. Cutting edge: efficient MHC class I cross-presentation during early vaccinia infection requires the transfer of proteasomal intermediates between antigen donor and presenting cells. J. Immunol. **171:**5668–5672.
62. **Shiver, J. W., T. M. Fu, L. Chen, D. R. Casimiro, M. E. Davies, R. K. Evans, Z. Q. Zhang, A. J. Simon, W. L. Trigona, S. A. Dubey, L. Huang, V. A. Harris, R. S. Long, X. Liang, L. Handt, W. A. Schleif, L. Zhu, D. C. Freed, N. V. Persaud, L. Guan, K. S. Punt, A. Tang, M. Chen, K. A. Wilson, K. B. Collins, G. J. Heidecker, V. R. Fernandez, H. C. Perry, J. G. Joyce, K. M. Grimm, J. C. Cook, P. M. Keller, D. S. Kresock, H. Mach, R. D. Troutman, L. A. Isopi, D. M. Williams, Z. Xu, K. E. Bohannon, D. B. Volkin, D. C. Montefiori, A. Miura, G. R. Krivulka, M. A. Lifton, M. J. Kuroda, J. E. Schmitz, N. L. Letvin, M. J. Caulfield, A. J. Bett, R. Youil, D. C. Kaslow, and E. A. Emini.** 2002. Replication-incompetent adenoviral vaccine vector elicits effective anti-immunodeficiency-virus immunity. Nature **415:**331–335.
63. **Sigal, L. J., S. Crotty, R. Andino, and K. L. Rock.** 1999. Cytotoxic T-cell immunity to virus-infected non-hematopoietic cells requires presentation of exogenous antigen. Nature **398:**77–80.
64. **Smith, C. L., P. R. Dunbar, F. Mirza, M. J. Palmowski, D. Shepherd, S. C. Gilbert, P. Coulie, J. Schneider, E. Hoffman, R. Hawkins, A. L. Harris, and V. Cerundolo.** 2005. Recombinant modified vaccinia Ankara primes functionally activated CTL specific for a melanoma tumor antigen epitope in melanoma patients with a high risk of disease recurrence. Int. J. Cancer **113:**259–266.
64a. **Smith, C. L., F. Mirza, V. Pasquetto, D. C. Tscharke, M. J. Palmowski, P. R. Dunbar, A. Sette, A. L. Harris, and V. Cerundolo.** 2005. Immunodominance of poxviral-specific CTL in a human trial of recombinant-modified vaccinia Ankara. J. Immunol. **175:**8431–8437.
65. **Steinman, R. M., D. Hawiger, and M. C. Nussenzweig.** 2003. Tolerogenic dendritic cells. Annu. Rev. Immunol. **21:**685–711.
66. **Subklewe, M., A. Chahroudi, A. Schmaljohn, M. G. Kurilla, N. Bhardwaj, and R. M. Steinman.** 1999. Induction of Epstein-Barr virus-specific cytotoxic T-lymphocyte responses using dendritic cells pulsed with EBNA-3A peptides or UV-inactivated, recombinant EBNA-3A vaccinia virus. Blood **94:**1372–1381.
67. **Sutter, G., and B. Moss.** 1992. Nonreplicating vaccinia vector efficiently expresses recombinant genes. Proc. Natl. Acad. Sci. USA **89:**10847–10851.
68. **Swedlow, J. R., J. W. Sedat, and D. A. Agard.** 1997. Deconvolution in optical microscopy, p. 284–307. *In* P. A. Jansson (ed.), Deconvolution of images and spectra. Academic Press, Inc., San Diego, Calif.
69. **Thornberry, N. A.** 1998. Caspases: key mediators of apoptosis. Chem. Biol. **5:**R97–R103.
70. **Tolonen, N., L. Doglio, S. Schleich, and J. Krijnse Locker.** 2001. Vaccinia virus DNA replication occurs in endoplasmic reticulum-enclosed cytoplasmic mini-nuclei. Mol. Biol. Cell **12:**2031–2046.
71. **Trevor, K. T., E. M. Hersh, J. Brailey, J. M. Balloul, and B. Acres.** 2001. Transduction of human dendritic cells with a recombinant modified vaccinia Ankara virus encoding MUC1 and IL-2. Cancer Immunol. Immunother. **50:**397–407.
72. **van Eijl, H., M. Hollinshead, and G. L. Smith.** 2000. The vaccinia virus A36R protein is a type Ib membrane protein present on intracellular but not extracellular enveloped virus particles. Virology **271:**26–36.
73. **Wasilenko, S. T., L. Banadyga, D. Bond, and M. Barry.** 2005. The vaccinia virus F1L protein interacts with the proapoptotic protein Bak and inhibits Bak activation. J. Virol. **79:**14031–14043.
74. **Wasilenko, S. T., T. L. Stewart, A. F. Meyers, and M. Barry.** 2003. Vaccinia virus encodes a previously uncharacterized mitochondrial-associated inhibitor of apoptosis. Proc. Natl. Acad. Sci. USA **100:**14345–14350.